

Microwave Spectrum of Acetyl Cyanide in the Ground and Excited States. I

F. Scappini * and H. Dreizler

Abteilung für Chemische Physik im Institut für Physikalische Chemie der Universität Kiel

(Z. Naturforsch. **31 a**, 840–846 [1976] ; received May 20, 1976)

The microwave spectra of acetyl cyanide, CH_3COCN , in the ground and in the two lowest excited states have been investigated. The rotational constants and the quadrupole coupling constants have been evaluated for all these states. The internal rotation parameters have been refined with respect to previous works. Evidence for a rotation–torsion–vibration interaction has been found in the spectra of the excited states.

I. Introduction

The rotation-torsion-vibration interaction has since long been of interest in this Laboratory and a model for molecules with a symmetry plane, allowing for two internal degrees of freedom has been developed^{1, 2}.

Methyl thiocyanate, CH_3SCN , and ethyl cyanide, $\text{CH}_3\text{CH}_2\text{CN}$, provided the first challenge to test the model^{3–6}. In $\text{CH}_3\text{CH}_2\text{CN}$ the closeness between the two lowest vibrational states, corresponding to the CCN-in-plane bending and to the methyl torsion, produces observable perturbations on their rotational spectra. In fact, while the ground state lines are unsplit, some lines in the first excited torsional state ($v_a, v_q = 1, 0$) and in the first excited CCN-in-plane bending state ($v_a, v_q = 1, 0$) exhibit splittings, which can not be interpreted by the usual rigid frame – rigid top theory. A model with two internal degrees of freedom, one for the methyl torsion and one for the in-plane bending, proved accurate enough to account for the measured spectra in this case and in the case of CH_3SCN .

It seemed reasonable to test further the model with other molecules⁷ and particularly with molecules having a barrier to the internal rotation low enough to allow for somewhat more split lines in the ground and in the excited states. Acetyl cyanide, in view of the previous studies^{8, 9} appeared to match our request.

In order to follow the sequence of the work done on acetyl cyanide we report in the present Part I the experimental results of the reinvestigation of the

ground state spectrum and of the investigation of the two lowest excited states, that is the (1,0)- and (0,1)-states. The hyperfine structure due to the N-quadrupole nucleus in the three states and the rotation-torsion interaction fine structure in the ground state are also discussed. The rotation-torsion-vibration interaction fine structure in the spectra of the two lowest excited states will be the subject of Part II¹⁰.

II. Experimental

The sample was made available to us by Fluka GmbH., Neu-Ulm, Germany, and was used after distillation.

Both Stark-effect spectroscopy and radiofrequency-microwave double resonance (RFMWDR) spectroscopy were extensively used in the present investigation. Microwave-microwave double resonance (MWMWDR) experiments were also performed to check some assignments. The corresponding instruments have been already described^{11–14}. Measurements were carried out in the region from 8 to 40 GHz at a temperature of about -50°C and at a pressure of about 5 mTorr.

III. Ground State Spectrum

With the published data not all the features of the ground state spectrum could be interpreted. In fact the transitions in the E torsional state (E transitions), connecting levels with high K_- value compared to J, did not occur within the predictions. Since these transitions are responsible for widely spaced A – E doublets, due to the effect of the linear terms in the Hamiltonian (1) of Section V, they are also very important for an accurate determination of the internal rotation parameters.

* On leave from Laboratorio di Spettroscopia Molecolare, Bologna, Italy.

Reprint request to Prof. Dr. H. Dreizler, Institut für Physikalische Chemie der Universität Kiel, Olshausenstraße 40–60, D-2300 Kiel, Germany.



Table 1. Ground state rotational spectrum of CH₃COCN. Frequencies are in MHz.

$J_{K-K+} - J'_{K'-K'+}$	State	$F - F'$	ν_{obs}	ν_{unsplit}^a	ν_{calc}^b	$(\nu_E - \nu_A)_{\text{obs}}$	$(\nu_E - \nu_A)_{\text{calc}}$
$1_{11} - 2_{12}$	A	1 - 2	13164.78	13165.85	13165.94	0.00	-0.24
		2 - 3	13166.09				
	E	1 - 2	13164.78	13165.85	13165.70		
		2 - 3	13166.09				
$1_{10} - 2_{21}$	A	2 - 3	33559.82	33560.01	33559.85	-5.76	-5.84
	E	2 - 3	33554.06	33554.25	33554.01		
$1_{01} - 2_{12}$	A	1 - 2	19193.98	19193.84	19194.06	-0.62	-0.74
		2 - 3					
	E	1 - 2	19193.36	19193.22	19193.32		
		2 - 3					
$2_{20} - 3_{21}$	A	1 - 2	22067.92	22066.90	22067.07	-4.13	-4.11
		2 - 3	22065.83				
		3 - 4	22067.25				
	E	1 - 2	22063.87	22062.77	22062.96		
		2 - 3	22061.63				
		3 - 4	22063.11				
$2_{12} - 3_{13}$	A	1 - 2	19660.33	19660.22	19660.25	-0.43	-0.43
		3 - 4					
	E	1 - 2	19659.90	19659.79	19659.82		
		3 - 4					
$2_{02} - 3_{13}$	A	3 - 4	24683.99	24683.91	24684.13	-0.48	-0.58
		2 - 3					
	E	3 - 4	24683.51	24683.43	24683.55		
		2 - 3					
$2_{02} - 3_{03}$	A	1 - 2	20895.26	20895.28	20895.12	-0.66	-0.71
		2 - 3					
		3 - 4					
	E	1 - 2	20894.60	20894.62	20894.41		
		2 - 3					
		3 - 4					
$2_{21} - 3_{22}$	A	2 - 3	21479.70	21480.88	21481.09	1.92	1.91
		3 - 4	21481.27				
	E	1 - 2	21483.84	21482.80	21483.00		
		2 - 3	21481.78				
		3 - 4	21483.10				
$3_{21} - 3_{30}$	A	2 - 2	32391.38	32392.02	32392.06	26.66	26.65
		4 - 4					
		3 - 3					
	E	2 - 2	32417.98	32418.68	32418.71		
		4 - 4					
		3 - 3					
$3_{22} - 3_{31}$	A	2 - 2	33115.48	33116.15	33116.19	-32.00	-31.79
		4 - 4					
		3 - 3					
	E	2 - 2	33083.33	33084.15	33084.40		
		4 - 4					
		3 - 3					
$3_{30} - 4_{31}$	A	3 - 4	28980.30	28981.32	28982.45	-18.67	-18.59
		4 - 5	28981.68				
	E	3 - 4	28961.71	28962.65	28963.86		
		4 - 5	28962.92				

Table 1 (continued)

$J_{K-K+} - J'_{K'-K'+}$	State	$F-F'$	ν_{obs}	ν_{unsplit}^a	ν_{calc}^b	$(\nu_E - \nu_A)_{\text{obs}}$	$(\nu_E - \nu_A)_{\text{calc}}$
$3_{31} - 4_{32}$	A	3-4	28906.76	28907.79	28908.93	15.89	15.73
		4-5	28908.16				
	E	3-4	28922.61	28923.68	28924.66		
		4-5	28924.09				
$3_{12} - 4_{13}$	A	2-3	30610.34	30610.35	30610.03	-1.83	-1.79
		3-4					
		4-5					
	E	2-3	30608.51	30608.52	30608.24		
		3-4					
		4-5					
$3_{03} - 4_{04}$	A	2-3	27268.33	27268.34	27268.34	-0.63	-0.69
		3-4					
		4-5					
	E	2-3	27267.70	27267.71	27267.65		
		3-4					
		4-5					
$3_{03} - 4_{14}$	A	2-3	29852.88	29852.90	29853.42	0.00	-0.38
		3-4					
		4-5					
	E	2-3	29852.88	29852.90	29853.04		
		3-4					
		4-5					
$3_{13} - 4_{04}$	A	2-3	23479.66	23479.66	23479.33	-0.82	-0.82
		3-4					
		4-5					
	E	2-3	23478.84	23478.84	23478.51		
		3-4					
		4-5					
$4_{22} - 4_{31}$	A	3-3	31476.94	31477.36	31478.37	10.17	10.37
		5-5					
		4-4					
	E	3-3	31487.12	31487.53	31488.74		
		5-5					
		4-4					
$4_{23} - 4_{32}$	A	3-3	33500.03	33500.41	33501.25	-15.37	-15.32
		5-5					
		4-4					
	E	3-3	33484.67	33485.04	33485.93		
		5-5					
		4-4					
$4_{23} - 5_{14}$	A	3-4	23529.36	23529.12	23527.92	-1.66	-1.62
		5-6					
		4-5					
	E	3-4	23527.68	23527.46	23526.30		
		5-6					
		4-5					
$6_{06} - 6_{15}$	A	5-5	24211.44	24211.55	24210.50	-6.09	-5.87
		7-7					
		6-6					
	E	5-5	24205.35	24205.46	24204.63		
		7-7					
		6-6					

Table 1 (continued)

$J_{K-K+} - J'_{K'-K'+}$	State	$F - F'$	ν_{obs}	$\nu_{\text{unsplit}}^{\text{a}}$	$\nu_{\text{calc}}^{\text{b}}$	$(\nu_{\text{E}} - \nu_{\text{A}})_{\text{obs}}$	$(\nu_{\text{E}} - \nu_{\text{A}})_{\text{calc}}$
$7_{16} - 7_{25}$	A	6-6	19939.53	19939.53	19941.22	-3.83	-3.70
		7-7					
		8-8					
	E	6-6	19935.70	19935.70	19937.52		
		7-7					
		8-8					
$7_{07} - 7_{16}$	A	6-6	30545.41	30545.52	30544.39	-7.67	-7.39
		8-8					
		7-7					
	E	6-6	30537.76	30537.85	30537.00		
		8-8					
		7-7					
$8_{17} - 8_{26}$	A	7-7	23716.82	23716.82	23718.56	-5.66	-5.55
		8-8					
		9-9					
	E	7-7	23711.16	23711.16	23713.01		
		8-8					
		9-9					
$8_{26} - 8_{35}$	A	7-7	25142.55	25142.55	25148.79	-1.00	-1.09
		8-8					
		9-9					
	E	7-7	25141.55	25141.55	25147.70		
		8-8					
		9-9					
$9_{27} - 9_{36}$	A	8-8	24901.74	24901.74	24909.04	-2.07	-2.26
		9-9					
		10-10					
	E	8-8	24899.67	24899.67	24906.78		
		9-9					
		10-10					
$9_{18} - 9_{27}$	A	8-8	28867.22	28867.22	28868.98	-7.80	-7.63
		9-9					
		10-10					
	E	8-8	28859.42	28859.42	28861.35		
		9-9					
		10-10					
$10_{28} - 10_{37}$	A	9-9	26012.16	26012.16	26020.33	-3.73	-4.08
		10-10					
		11-11					
	E	9-9	26008.43	26008.43	26016.25		
		10-10					
		11-11					
$11_{29} - 11_{38}$	A	10-10	28686.43	28686.43	28695.05	-5.98	-6.43
		11-11					
		12-12					
	E	10-10	28680.45	28680.45	28688.62		
		11-11					
		12-12					
$12_{210} - 12_{39}$	A	11-11	32987.37	32987.37	32995.93	-8.64	-9.03
		12-12					
		13-13					
	E	11-11	32978.73	32978.73	32986.90		
		12-12					
		13-13					

^a Hyperfine center frequency calculated with the constants from Table 2.^b Calculated with the Hamiltonian (1) and the constants from Table 5.

Some A–E doublets of this type were searched for and assigned using the RFMWDR technique and/or their characteristic Stark effect. An example of radiofrequency-microwave double resonance connections is shown in Fig. 1, for the same A and E rotational levels.

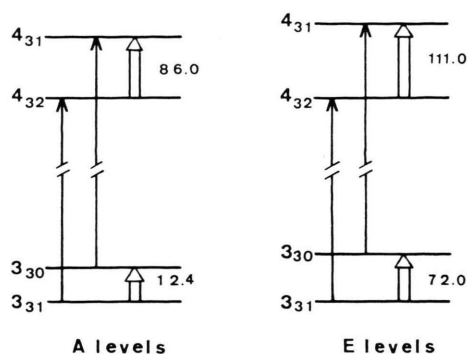


Fig. 1. Example of radiofrequency — microwave double resonance connections in the ground state. The drawings are not to scale. The rotational energies of A levels are considerably different from those of E levels, resulting in different pumping and signal frequencies (MHz).

In the case of the E transitions both the pump and the signal frequency had to be located by a double search procedure. Spectra at a Stark field of the order of a few V/cm provided also an efficient tool to identify this type of transitions, as they are in general very sensitive to Stark modulation.

The hyperfine structure of the lines was resolved whenever the two components of the internal rotation doublets were separated enough to prevent overlapping among the hyperfine structure satellites.

The measured transitions, including those re-measured with better accuracy and resolution than in Reference⁸, are listed in Table 1. The effective rotational constants for the A ground state were calculated by a least squares-rigid rotor fit to the A transitions up to $J=3$. No centrifugal distortion correction was necessary within the experimental errors. From the hyperfine structure the N-quadrupole coupling constants were obtained. They resulted equal, within the experimental uncertainties, for the A and E states. Using the structure given in Reference⁸ and assuming the z -principal axis of the nuclear quadrupole coupling tensor collinear with the $C\equiv N$ bond, while the y -axis is perpendicular to the molecular symmetry plane, the diagonal (and principal) elements are also determined. The cal-

Table 2. Effective rotational constants for the ($v_a, v_q=0,0$) — A state, obtained from transitions up to $J=3$. Out-of-plane contribution $I_a+I_b-I_c$. Nuclear quadrupole coupling constants. Quoted standard errors.

A_A	=	10185.67	± 0.03	MHz
B_A	=	4157.57	± 0.03	MHz
C_A	=	3002.77	± 0.02	MHz
$I_a+I_b-I_c$	=	2.8687		amu·Å ²
χ_{aa}	=	-4.34	± 0.07	MHz
χ_{bb}	=	2.03	± 0.31	MHz
χ_{cc}	=	2.31	± 0.31	MHz
χ_{xx}	=	2.06		MHz
χ_{yy}	=	2.31		MHz
χ_{zz}	=	-4.37		MHz
η	=	0.06		

culated value of the asymmetry parameter $\eta = (\chi_{xx} - \chi_{yy})/\chi_{zz}$ indicates that the charge distribution around the $C\equiv N$ bond is almost cylindrically symmetric. The results are given in Table 2.

IV. Excited States Spectra

Each ground state transition of acetyl cyanide is accompanied by detectable satellites due to transitions in the excited states. By a few low resolution spectra, using the procedure as for the ground state, we were able to identify two sets of doublets from the two lowest excited states. General feature of the $3_{13}-4_{04}$ transitions is illustrated in Figure 2. Infra-

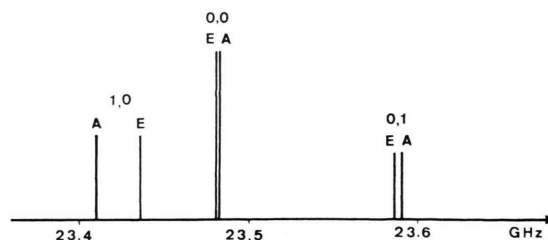


Fig. 2. The $3_{13}-4_{04}$ transitions in CH_3COCN .

red and Raman spectra were run at the same time and a vibrational analysis¹⁰ was performed to parallel the microwave findings. These two vibrational modes can be described as the torsion of the methyl group and the in-plane bending of the CCN group. Assignment of the rotational spectrum to the proper vibrational state was based on the relative intensities of corresponding transitions, on consideration of the inertial defect¹⁵, and on the splittings of the A–E doublets.

a) CH_3 -torsion

The lowest fundamental vibration was calculated from the V_3 -value (see below) to be at $131.5 \pm 1.5 \text{ cm}^{-1}$. Relative intensity measurements of the rotational lines agree with this result. Moreover the decrease in the inertial defect compared to that in the ground state is in accordance with the general trend for an out-of-plane vibration. Further support comes also from the vibrational analysis¹⁰.

The rotational spectrum exhibits widely separated A–E doublets. The correct assignment of the A transitions was established by a rigid rotor fit. A detailed account of the measured transitions will be given in Part II¹⁰, together with an analysis of the A–E splittings.

Final values of the effective rotational constants for the A state were obtained by a least squares fit to the transitions up to $J=3$. No centrifugal distortion correction was necessary within the experimental errors. The hyperfine structure analysis led to the N-quadrupole coupling constants with no meaningful differences between the A and E states. The values obtained are collected in Table 3.

Table 3. Effective rotational constants for the $(v_a, v_q=1,0)$ – A state, obtained from transitions up to $J=3$. Out-of-plane contribution $I_a+I_b-I_c$. Nuclear quadrupole coupling constants. Fundamental frequency. Quoted standard errors.

A_A	=	10174.91	± 0.03 MHz
B_A	=	4141.75	± 0.03 MHz
C_A	=	3000.75	± 0.02 MHz
$I_a+I_b-I_c$	=	3.2722	$\text{amu} \cdot \text{\AA}^2$
χ_{aa}	=	-4.72	± 0.07 MHz
χ_{bb}	=	1.14	± 0.15 MHz
χ_{cc}	=	3.58	± 0.15 MHz
$\nu(v_a, v_q=0,0-1,0)^a$	=	131.5	$\pm 1.5 \text{ cm}^{-1}$

^a Calculated from the V_3 -value.

b) CCN In-plane Bending

The increase in the inertial defect respect to that in the ground state indicates that the second lowest fundamental is an in-plane vibration. By liquid phase Raman spectra it is identified at $191 \pm 1 \text{ cm}^{-1}$. This value is not far from that of the CCN-in-plane bending of ethyl cyanide at $206.5 \pm 1.5 \text{ cm}^{-1}$ (see⁵). Relative intensity measurements of rotational lines are in agreement with this result.

The rotational spectrum presents A–E doublets, whose separations are different from the corresponding ones in the ground state. The assignment of the

Table 4. Effective rotational constants for the $(v_a, v_q=0,1)$ – A state, obtained from the transitions up to $J=3$. Out-of-plane contribution $I_a+I_b-I_c$. Nuclear quadrupole coupling constants. Fundamental frequency. Quoted standard errors.

A_A	=	10158.02	± 0.03 MHz
B_A	=	4176.19	± 0.03 MHz
C_A	=	3005.56	± 0.02 MHz
$I_a+I_b-I_c$	=	2.6180	$\text{amu} \cdot \text{\AA}^2$
χ_{aa}	=	-4.15	± 0.09 MHz
χ_{bb}	=	2.01	± 0.24 MHz
χ_{cc}	=	2.14	± 0.24 MHz
$\nu(v_a, v_q=0,0-0,1)^a$	=	191	$\pm 1 \text{ cm}^{-1}$

^a From liquid phase Raman spectra.

A transitions was confirmed by a rigid rotor fit. A list of the measured transitions will be found in Part II¹⁰.

Final values of the effective rotational constants for the A state together with the N-quadrupole coupling constants were obtained as described in the Section above. Results are given in Table 4.

V. Analysis

In this work we are only concerned with the analysis of the rotation-torsion interaction in the ground state spectrum. The vibration interaction manifests itself only in the excited states spectra.

The effective Hamiltonian that we have used to fit the ground state transitions is expressed, in the principal axis system, as¹⁶:

$$H_{v_0} = A P_a^2 + B P_b^2 + C P_c^2 + F \sum_{n=1}^2 W_{v_0}^{(n)} \cdot \left(\lambda_a \frac{I_a}{I_a} P_a + \lambda_b \frac{I_b}{I_b} P_b \right)^n \quad (1)$$

where P_a , P_b , and P_c are the total angular momentum operators (the c axis is perpendicular to the molecular symmetry plane),

$$F = \frac{1}{2} \frac{\hbar^2}{r I_a}, \quad r = 1 - \lambda_a^2 \frac{I_a}{I_a} - \lambda_b^2 \frac{I_b}{I_b}, \quad \lambda_a \text{ and } \lambda_b$$

are the direction cosines between the symmetry axis of the top and the principal axes a and b respectively (in this case is $\lambda_c=0$), $W_{v_0}^{(n)}$ are the n -th order perturbation coefficients which depend on the reduced barrier height $s = \frac{4}{9} \frac{V_3}{F}$, and I_a is the moment of inertia of the top about its symmetry axis.

Of the six internal rotation parameters involved in the Hamiltonian (1), I_a was fixed to the value of

3.14 amu·Å² from Reference⁸. The effect of I_a on the A–E splittings is correlated to that of V_3 and only the reduced barrier height s is obtained from the analysis. The other five parameters A , B , C , V_3 , and λ_a were obtained by using the frequencies of the measured transitions. The rotational constants were fit only to the lines up to $J=3$, while the remaining parameters V_3 and λ_a were determined from the splittings of all the measured transitions. The parameters which enter in the Hamiltonian (1) are given in Table 5. The A and E transition frequencies, calculated by using these parameters, are compared with the observed values in Table 1. The uncertainty on I_a (± 0.04 amu·Å²), which comes from the structure, has been accounted for in the estimation of the errors on the fitted parameters.

Table 5. Parameters in the Hamiltonian (1) obtained by the fit to the ground state transitions. The uncertainty on I_a comes from the structure⁸. The errors on the other parameters follow from the error propagation law.

A	=	10185.22	± 0.03	MHz
B	=	4157.36	± 0.03	MHz
C	=	3002.79	± 0.02	MHz
I_a	=	(3.14 ± 0.04) ^a		amu·Å ²
λ_a	=	0.5155	± 0.0040	
V_3	=	1207	± 16	cal/mole
s	=	33.68	± 0.06	
F	=	166.97	± 2.02	GHz

^a Taken from Reference⁸.

VI. Conclusion

The angle between the top axis and the a-axis obtained from the internal rotation analysis indicates that the methyl group is tilted toward the double bond by about 2°. This situation had already been pointed out by Nelson et al.⁹

The calculated frequency of the methyl torsion at 131.5 cm⁻¹ and the identification of the in-plane CCN bending at 191 cm⁻¹ are not in accordance with a previous work¹⁷. The experimental evidence for the methyl torsion seems to be confined to the far infrared region, where intensity problems are to be expected, since a search for combination bands between torsion and methyl stretching or deformation was unsuccessful.

The calculated barrier height does not differ sensitively from the values obtained in References^{8,9}. Mainly the refinements of the other internal rotation parameters have led to a more satisfactory prediction of the ground state spectrum.

With the value of the barrier height from the ground state splittings it is not possible to account for the splittings in the (1,0)-state, not even including a V_6 term in the potential function. Moreover the splittings in the (0,1)-state are different from the corresponding ones in the ground state, while in a rigid frame-rigid top approximation they should be equal. These facts lead to the conclusion that a rotation-torsion-vibration interaction occurs and a molecular model with, at least, two internal degrees of freedom has to be considered in order to interpret all measured spectra. The present measurements of excited states transitions appear of importance for the further interaction analysis.

VII. Acknowledgements

The authors want to thank Dr. H. Mäder, Dipl.-Chem. H. Lutz, and W. Schrepp for cooperation, and Prof. D. Sutter for comments. The research funds and the research grant (F.S.) of the "Deutsche Forschungsgemeinschaft" and of the "Fonds der Chemie" are acknowledged. Calculations have been made with the PDP 10 computer of the "Rechenzentrum der Universität Kiel".

¹ H. Dreizler, Z. Naturforsch. **23 a**, 1077 [1968].

² H. Mäder, U. Andresen, and H. Dreizler, Z. Naturforsch. **28 a**, 1163 [1973].

³ H. Dreizler and A. M. Mirri, Z. Naturforsch. **23 a**, 1313 [1968].

⁴ U. Andresen and H. Dreizler, Z. Naturforsch. **29 a**, 797 [1974].

⁵ H. Mäder, H. M. Heise, and H. Dreizler, Z. Naturforsch. **29 a**, 164 [1974].

⁶ H. M. Heise, Thesis, University of Kiel, Kiel, Germany, 1976.

⁷ M. Kuhler, L. Charpentier, D. Sutter, and H. Dreizler, Z. Naturforsch. **29 a**, 1335 [1974].

⁸ L. C. Krisher and E. B. Wilson, J. Chem. Phys. **31**, 882 [1959]; erratum **33**, 304 [1960].

⁹ R. Nelson and L. Pierce, J. Mol. Spectrosc. **18**, 344 [1965].

¹⁰ Part II, to be published.

¹¹ U. Andresen and H. Dreizler, Z. Angew. Phys. **30**, 207 [1970].

¹² R. Schwarz, Thesis, University of Kiel, Kiel, Germany, 1974.

¹³ F. Scappini and A. Guarnieri, Z. Naturforsch. **27 a**, 1011 [1972].

¹⁴ G. K. Pandey and H. Dreizler, Z. Naturforsch. **31 a**, 357 [1976].

¹⁵ D. R. Herschbach and V. W. Laurie, J. Chem. Phys. **40**, 3142 [1964].

¹⁶ H. Dreizler, Fortsch. Chem. Forsch. **10**, 59 [1968].

¹⁷ M. Sugiè and K. Kuchitsu, J. Mol. Struct. **20**, 437 [1974].